Journal of Information Systems Engineering and Management
2025, 10(9s)
e-ISSN: 2468-4376
https://www.jisem-journal.com/

Research Article

Analysis of PI and Hysteresis Controlled Cascaded Dual loop Quadratic -Boost-Multilevel Inverter System

Neelashetty Kashappa
[1] *Faculty, EEE department, Guru Nanak Dev Engineering College, Bidar*
Karnataka-585401
neelshettyk@gmail.com

ARTICLE INFO

Received: 28 Oct 2024

Revised: 20 Dec 2024

Accepted: 02 Jan 2025

ABSTRACT

Quadratic Boost Converter (QBC) finds a place between PV and single phase Multi Level Inverter (MLI) with motor load. In this work, we devise a new QBC between DC source and nine-levels MLI. A Hysteresis Controller (HC) and PI have been considered for the closed loop response of QBC-MLI system. The key finding of proposed system is evaluating and differentiate dynamic response of closed two-loop PI-PI & PI-HC controlled QBC-MLI systems and output current THDs. The computer simulation using MATLAB software demonstrates efficient and dynamic performance of the HC controlled QBC-MLI system. Efficacy of proposed system is authenticated through the simulation outcomes.

Keywords: QBC (Quadratic-Boost-Converter), MLI-NL (MLI with Nine Levels), THD (Total Harmonic Distortion), PI controller, HC, Single Phase IM (Induction Motor), Time domain characteristics

INTRODUCTION

In order to defeat the constraints of different converters in SPV-array, a QBC was adapted which is a DC–DC-QBC, which is evaluated by an-Canonical-Switching-Converter (CSC) [4] or topological variations upon DC-DC-QBC [5]. An acquiesce inductor causes a shift in CSC, which in turn causes a QBC [1-3]. CSC converter is hindered by large current ripples in input and capitulate flows. A true Switched-Mode (SM) topology is produced by increasing little inductance at output of this conversion step. This leads to a DC-connect low-yield ripple current. When compared to other DC-DC converters, LC provides best overall system performance. Ordinary Buck-Boost Converter (BBC) is widely used due to Simplicity. However, it shows the increased input and output current ripples. The presented LC yield the reduced ripples in the current and shows a remarkable trade-off input-current- ripples.

Induction motors are widely employed in industry since they are reasonable, rugged, and do not need any assistance. Over half of world's electrical energy output goes toward powering electric devices. In order to save money and lessen environmental pollution, it is essential to improve the efficiency of electric drives [6, 7]. As far as measured speed and torque are concerned, induction motors perform well. Whatever case may be, engine's efficiency drops dramatically under low loads due to copper's difficulty with center-faults. As a result, reducing engine power consumption is as simple as adjusting transition level. [8, 9]. Among the many uses for induction motors are those in HVAC, industrial drives (for movement control and robotics), controlling in EV's, and many more [10]. A number of operational capabilities govern induction motor drives (IMDs), including input control, velocity, torque, air gap movement, power factor, stator current or voltage, and overall efficiency. [11]. 3-phase induction motor is often utilized in mechanical applications due to its relatively low effort, free assistance, and elevated-steadfast quality. In contrast, single-phase motor is more commonly found in electrical home appliances like air blowers, centrifugal syphons, electric fans, etc, and is typically connected to 3-phase electrical system. [12][13].

With development of intensity devices, induction motors (IMs) can be used for constant speed applications where voltage source frequency is constant, or for variable speed applications where frequency and voltage are both variable, by establishing 3-phase supply with PWM procedures linked to SSI. Relatively simple construction, support-free activities, and ability to start directly from supply organ of three-stage IMs (induction motors) have made them widely

used in boost and automobile applications for quite some time. FOC (Field-Orientation-Control) is responsible for enrollment machine's top-notch features. An Induction FOC system was shown, which consists of 3 stages and uses complex exchange work concept to tune PI-controller. This system makes use of controlled-IM's recurrent response capacity and closed-loop complex exchange capacity.

RESEARCH GAP

Use of motors for AC loads is not mentioned in the aforementioned publications. This study recommends using a motor for alternating current loads. No discussion of AC loads in closed-loop regulated QBC-MLI systems using PI-PI and PI-HC controllers is found in the aforementioned literature. Using PI and HC controllers, this study compares the QBC-CMLI system for AC loads.

SYSTEM DESCRIPTION

Fig-1 portrays block diagram of closed-loop QBC-MLI system controlled by a PI-PI device.

Basic -equation of QBC voltage ratio

$$V_o = V_1 T_{on}/ T \qquad (1)$$

Where, V_o = Output voltage,
V_i = Input voltage,
T_{on} = On time,
T = Total time

$$T_{on} = Vo\ T/V_i \qquad (2)$$
$$E_{pr} = KN_1P_f \qquad (3)$$
$$E_{se} = KN_2P_f \qquad (4)$$

Controller's representation is derived from differentiation of motor speed and current. To get error signal, we measure DC-yield-voltage and compare it to reference-yield-voltage. In order to keep motor speed constant and reduce steady-state error, PI courses this error signal. Real speed is contrasted with set-speed. Proportional-gain (K_p) and double-integral-times (T_{is}) PI parameters are evaluated with the use of Zeigler Nichols tuning technique.

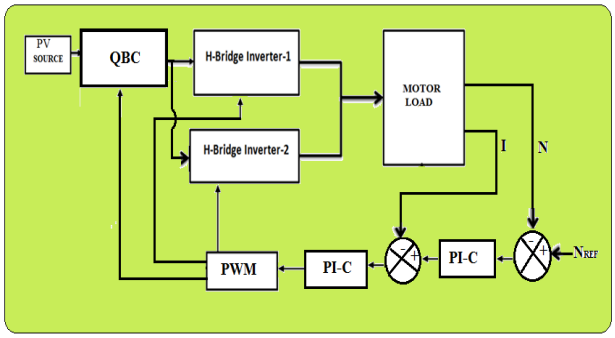

Fig.1 Block diagram of QBC-MLI system with PI-PI controller.

Fig-2 shows a block schematic of a closed-loop QBC-MLI system that uses HC controllers. Error signal is produced by sensing and evaluating dc-yield-voltage with reference-yield-current and motor speed. In order to maintain a consistent output motor speed and reduce steady-state error, HC courses this error signal.

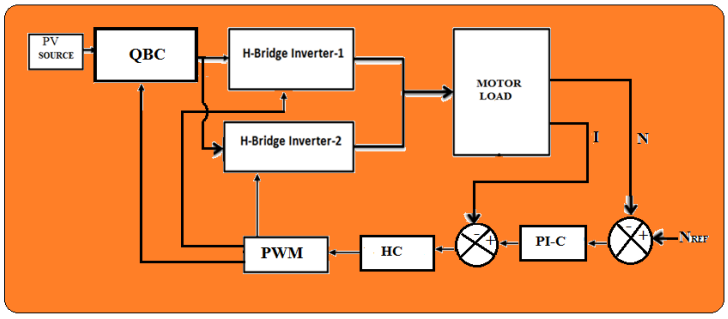

Fig.2 Block diagram of QBC-MLI system with PI-HC controller.

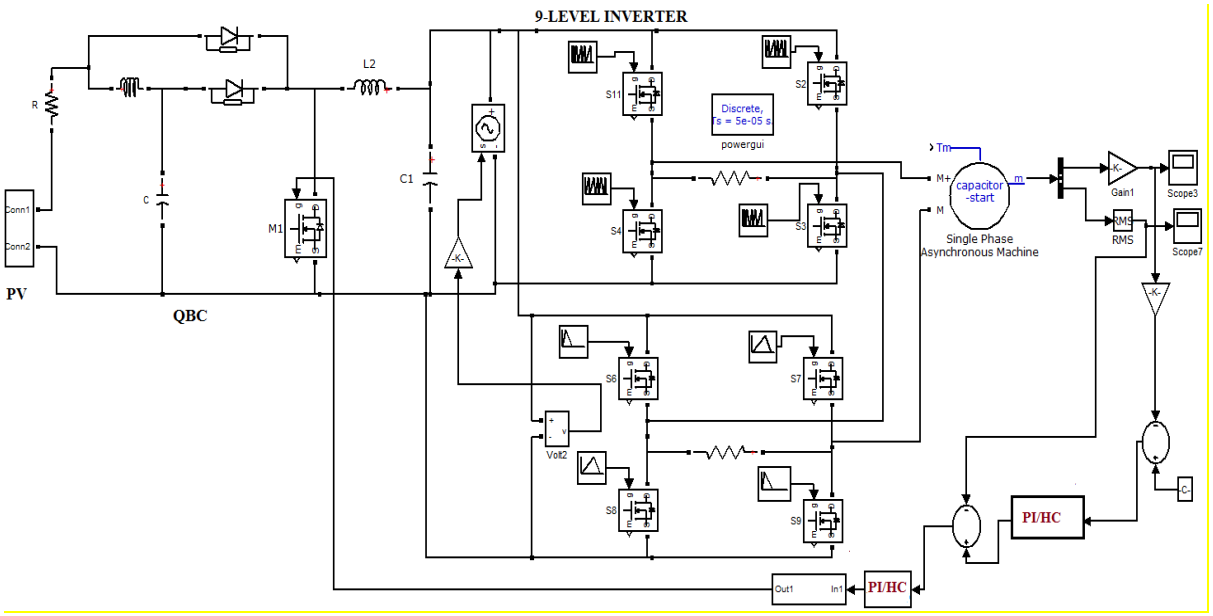

Fig.3 Circuit diagram of closed loop QBC-MLI system with PI and HC controllers

Figure 3 shows schematic of a closed 2-loop QBC-MLI system for a DC-AC converter operating under motor load. Goal is to meet applicable standard while improving motor speed management and reducing current total harmonic distortion (THD). In order to validate the QBC and MLI systems under PI and HC control, output current string is regulated using speed and current regulators. Focusing upon QBC-CMLI system of AC-DC converters with motor load networks, this research aims to minimize output current THD and regulate speed.

RESULTS AND DISCUSSION

1. Open loop QBC-MLI system with source disturbance

An open-loop source disturbance circuit schematic Figu-4 portrays QBC-MLI system. An open-loop QBC-MLI system's input voltage is shown in Fig. 5. An increase from 75V to 80V is made to the voltage across PV. Figure 6 shows the QBC-MLI system's output voltage, which is 160V. As portrayed into fig-7, QBC-MLI system has an output voltage of 160V across the motor load. As shown in Figure 8, the QBC-MLI system has output current of 5A. Figure 9 shows output current THD of motor load, which is 6.94%. Figure 10 shows QBC-MLI system's motor speed, which is 1250 rpm. Figure 11 shows QBC-MLI system's motor torque, which is 1.56 N-m.

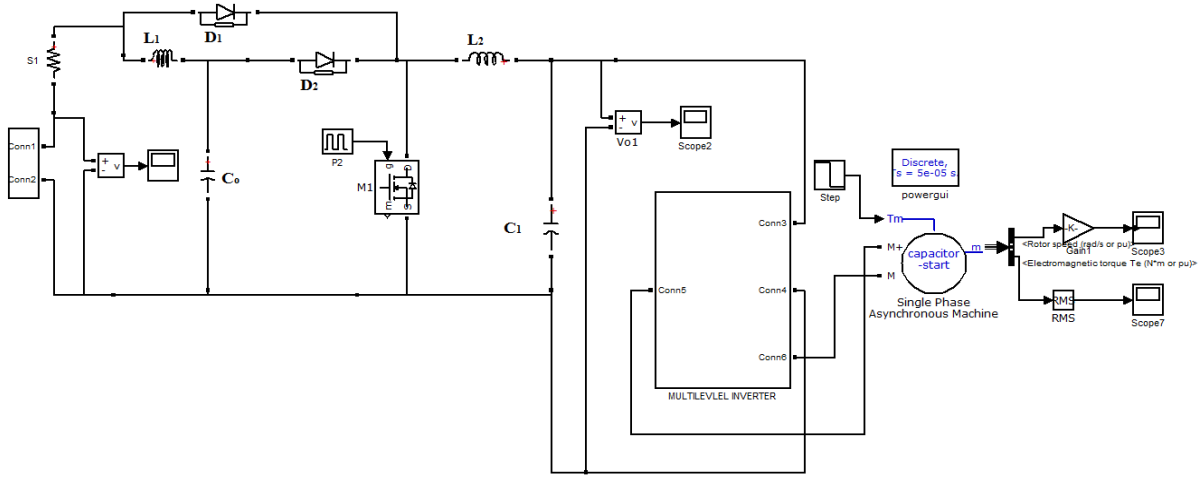

Fig.4 Circuit diagram of open loop QBC-MLI system with source disturbance

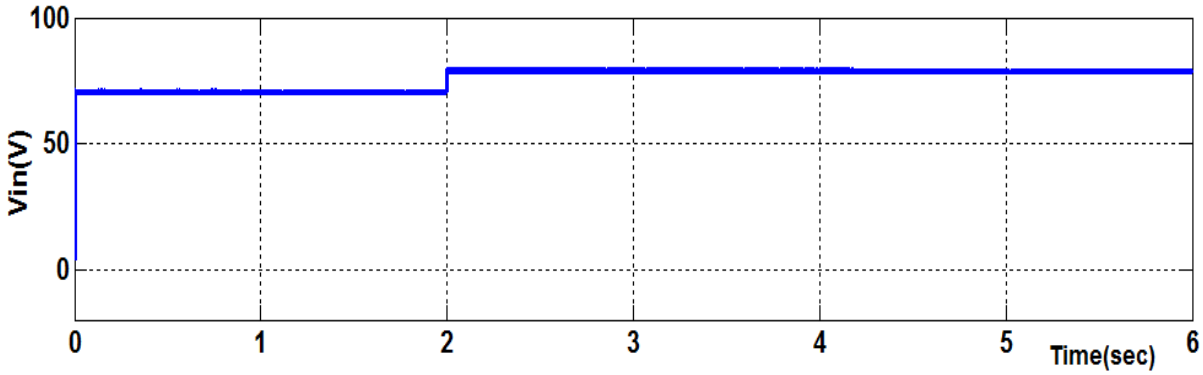

Fig. 5 Voltage across PV

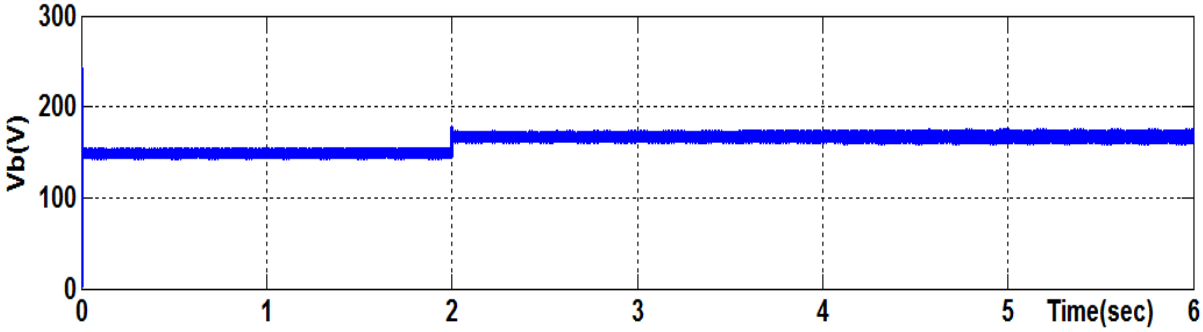

Fig.6 Output voltage across QBC-MLI system with source disturbance.

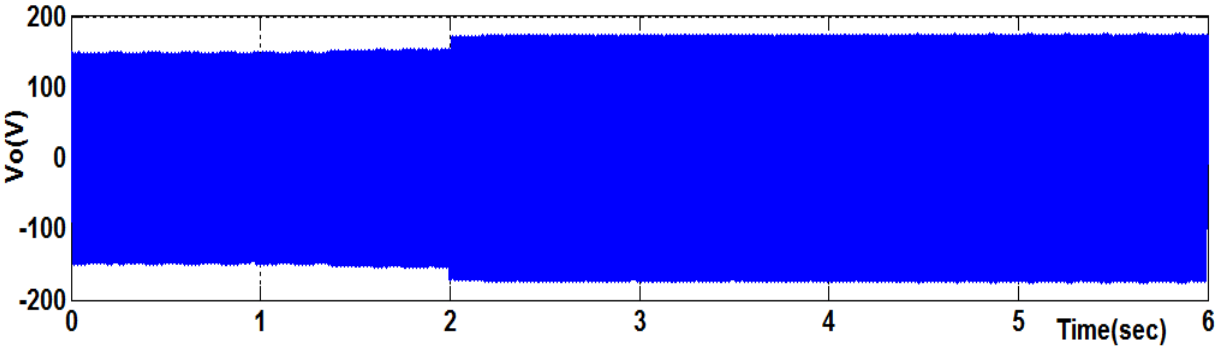

Fig.7 Output voltage across motor of open loop QBC-MLI system with source disturbance.

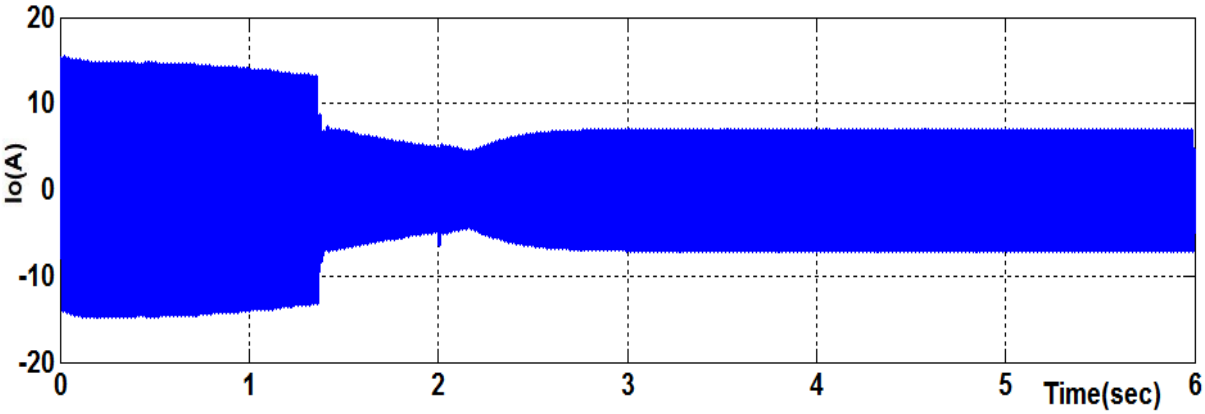

Fig. 8 Output current through the open loop QBC-MLI system with source disturbance.

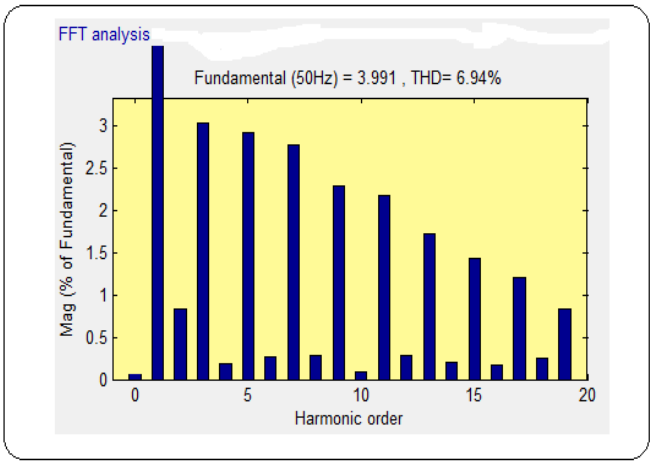

Fig.9 Output current THD with source disturbance

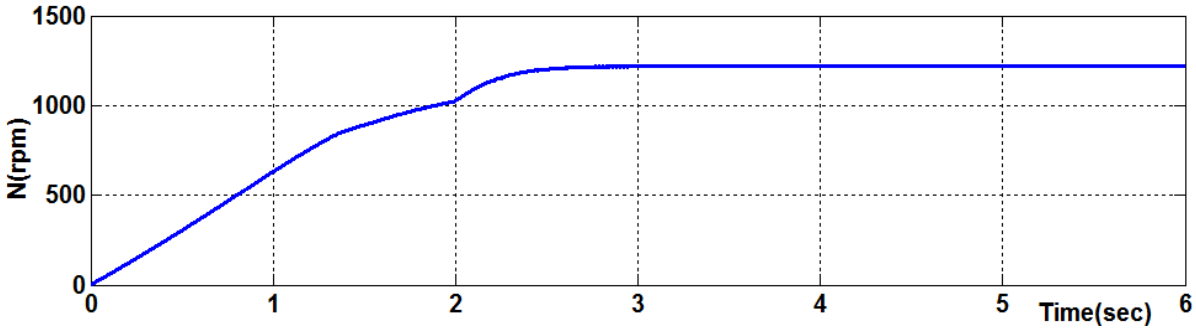

Fig.10 Motor speed of open loop QBC-MLI system with source disturbance

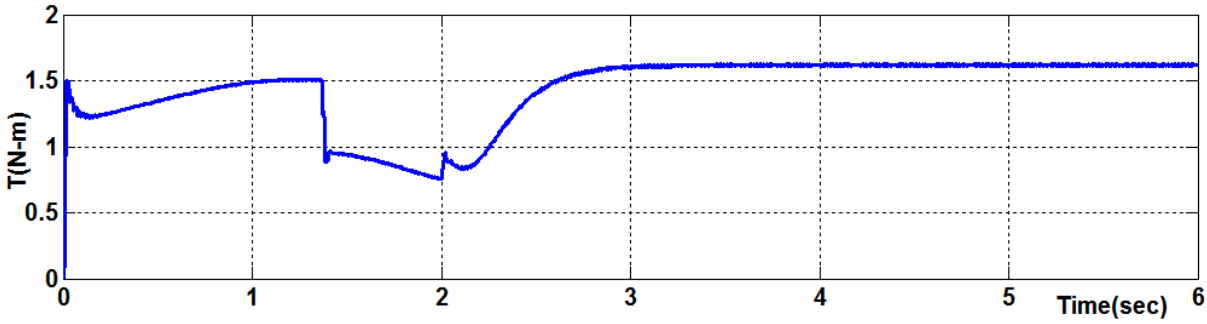

Fig.11 Motor torque of open loop QBC-MLI system with source disturbance.

2. QBC-MLI system with closed two-loop PI controller

Fig-12 shows wiring schematic of a closed two-loop Quadratic Boost-Conveter with Multi Level Inverter (QBC-MLI) using a PI-PI controller. Fig-13 portrays input voltage through PV. An increase from 75V to 80V is made to the voltage across PV. Figure 14 shows the QBC-MLI system's output voltage. The output voltage has value of 150V. Figure 15 shows voltage across motor load. Throughout motor load, voltage is 150V. Figure 16 portrays current flowing via motor load. Through motor load, the current is 4.2A. Figure 17 portrays output current THD of motor load, which is 5.34 percent. In Fig.18, motor speed is shown, and it's 1100 rpm. The motor torque, which is portrayed into fig-19, has a value of 0.9 N-m.

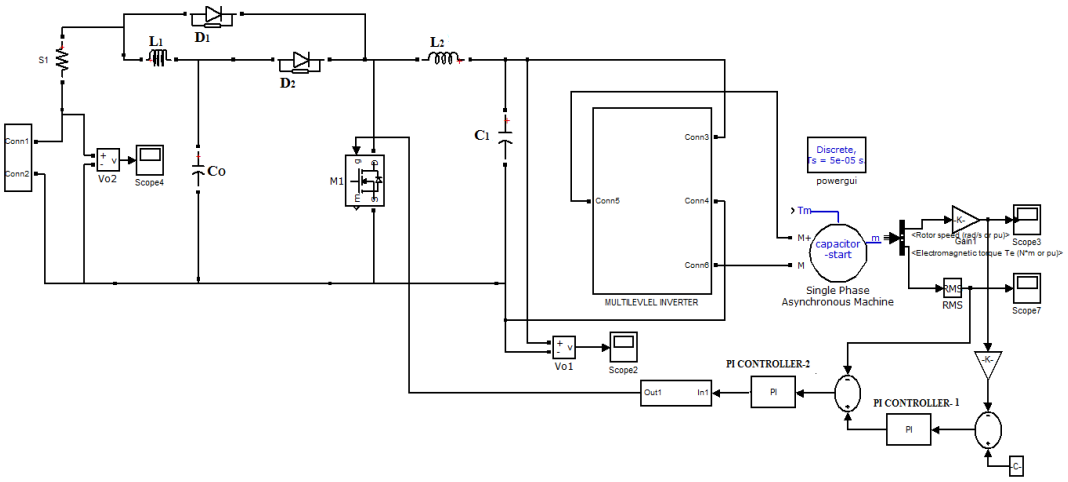

Fig.12 Circuit diagram of closed two-loop QBC-MLI system with PI-PI controller.

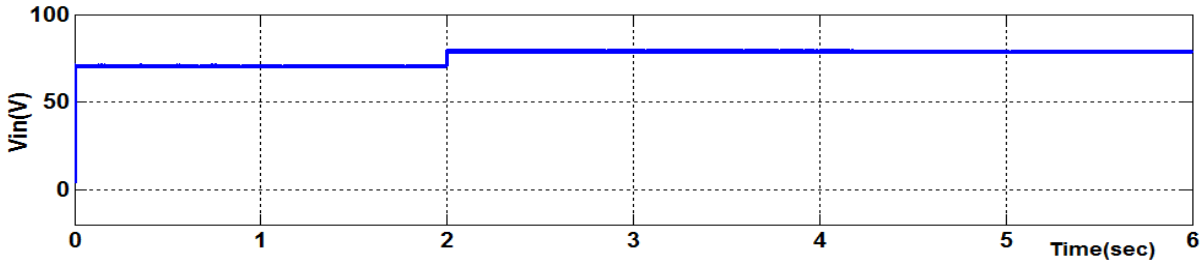

Fig.13 Voltage across PV

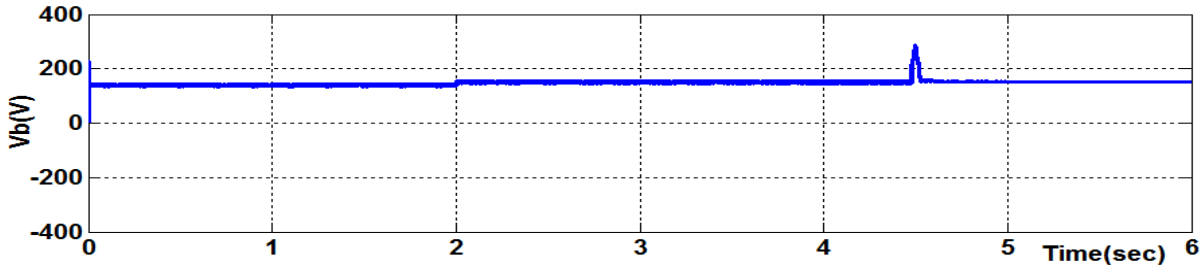

Fig.14 Output voltage across closed two-loop QBC-MLI system with PI-PI controller.

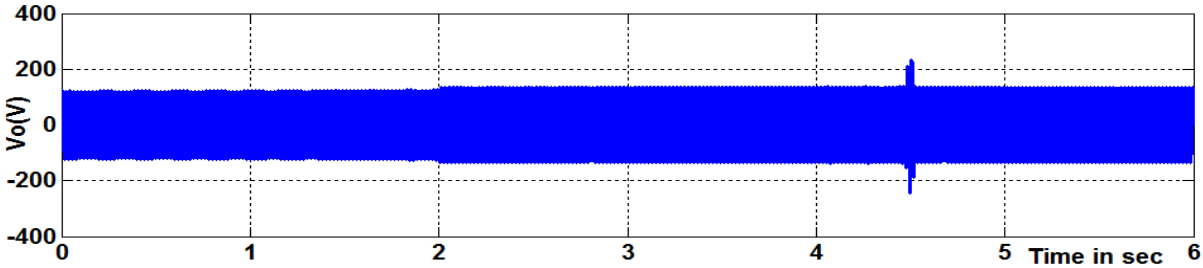

Fig.15 Output voltage across motor of closed two-loop QBC-MLI system with PI-PI controller

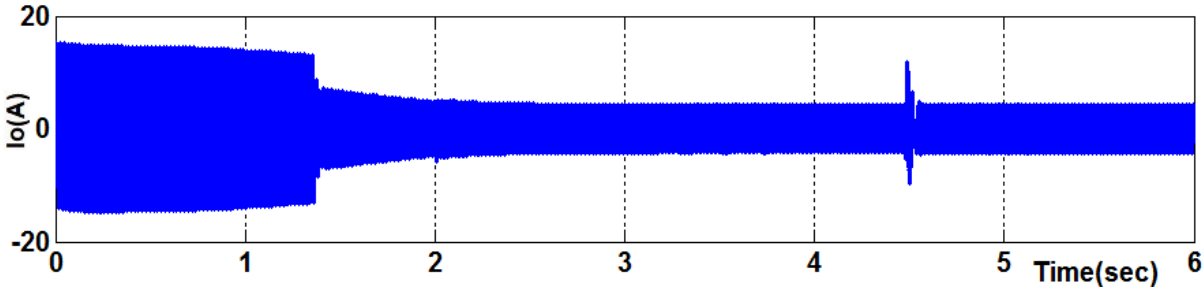

Fig.16 Output current through closed two-loop QBC-MLI system with PI-PI controller.

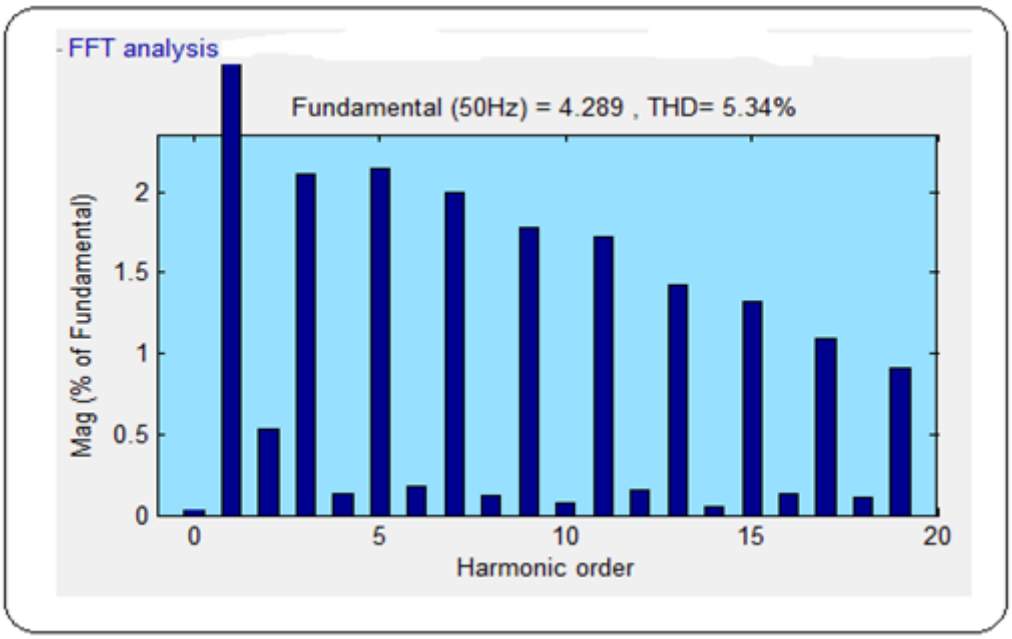

Fig.17 Output current THD with PI-PI Controller

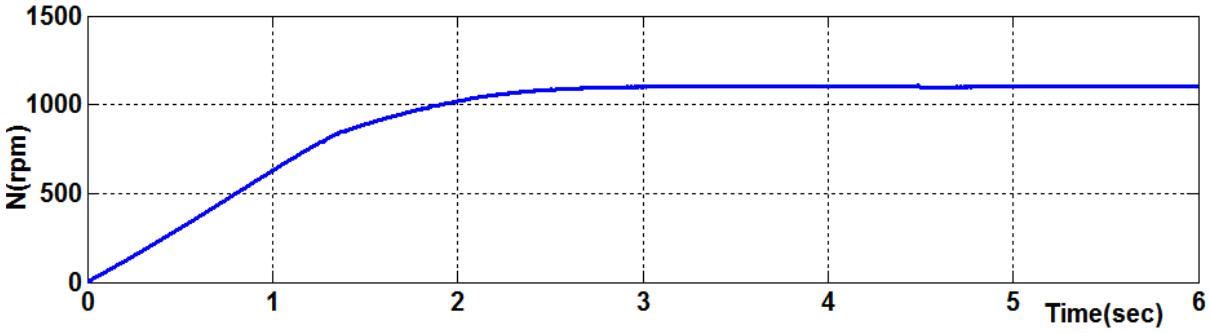

Fig.18 Motor speed of closed two-loop QBC-MLI system with PI-PI controller**.**

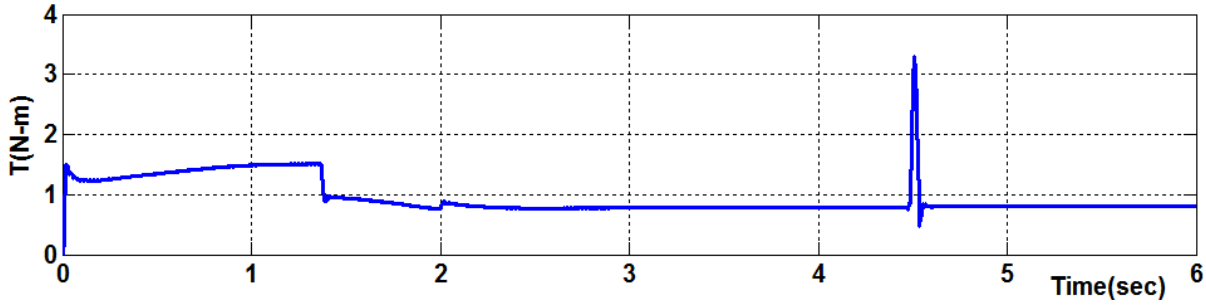

Fig.19 Motor torque of closed two-loop QBC-MLI system with PI-PI controller.

3. QBC-MLI system with closed two-loop HC controller

Figure 20 is a schematic depicting a closed two-loop QBC-MLI using a PI-HC controller. On the other hand, Figure 21 shows input voltage across PV. An increase from 75V to 80V is made to voltage across PV. Figure 22 shows QBC-MLI system's output voltage, which is 150V. The value of voltage across the motor load is 150V, as shown in Fig.23. Fig-24 shows zoomed-out output voltage over motor load. Value of the current through motor load is 16A, as shown in Fig-25. In Fig.26, we can see zoomed-out output current coming via the motor load. Fig.27 shows the motor load's output current THD, which is 4.40%. Figure 28 shows the motor's speed, while Figure 29 shows its zoom out. One hundred and hundred revolutions per minute is the value of motor speed. Figures 30 and 31 show the motor torque and its zoom out, respectively. Motor torque measures 0.9 N-m.

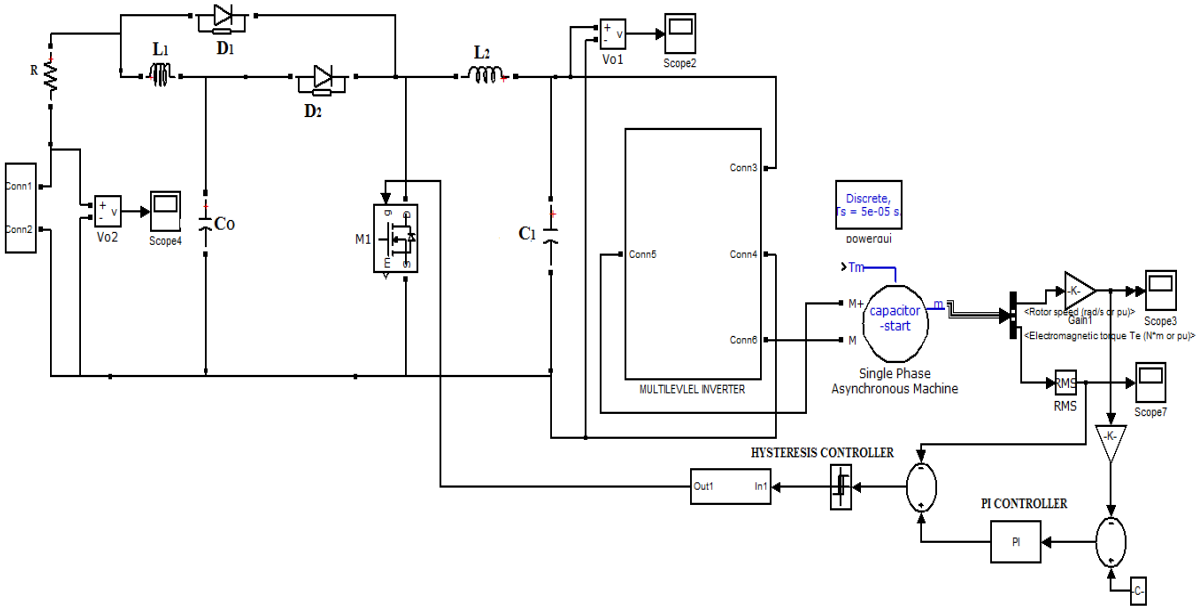

Fig.20 Circuit diagram of closed two-loop QBC-MLI system with PI-HC controller

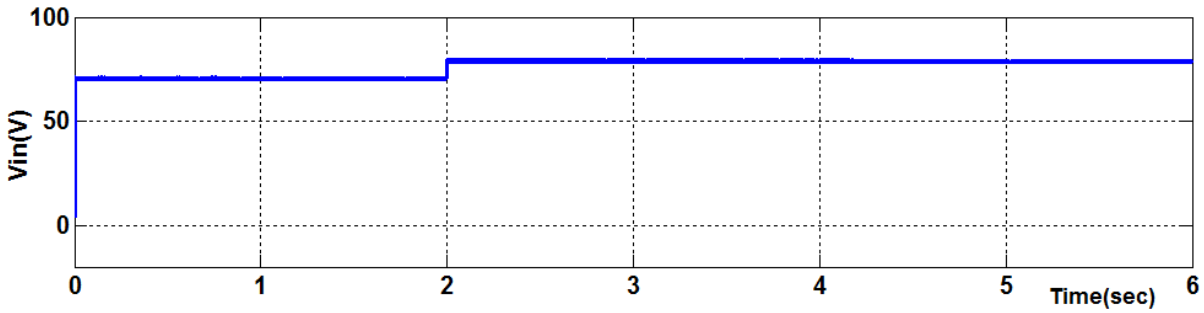

Fig.21 Voltage across PV.

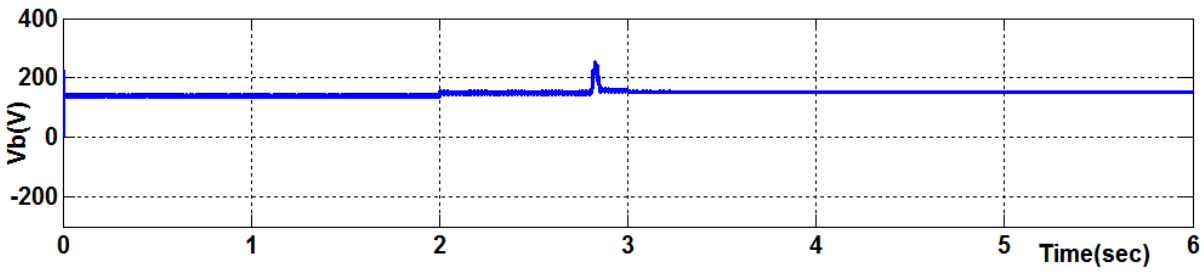

Fig.22 Output voltage across QBC-MLI system with PI-HC controller.

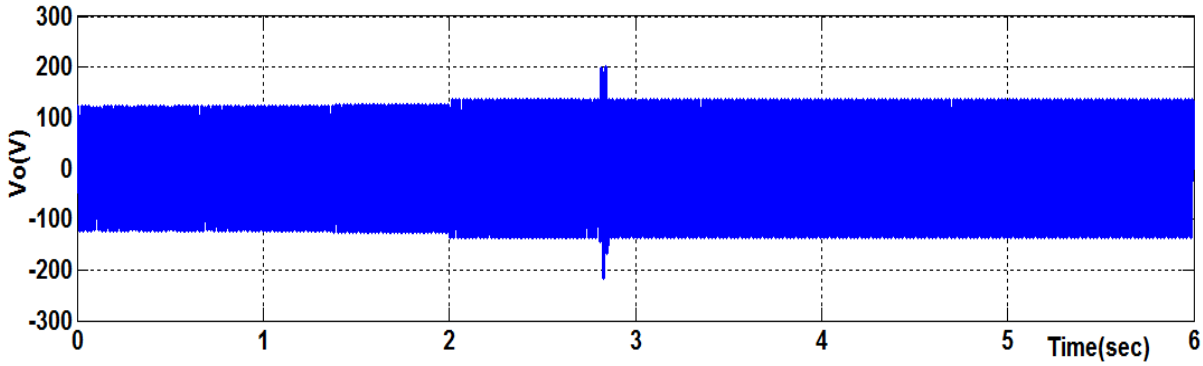

Fig.23 Output voltage across motor of closed two-loop QBC-MLI system with PI-HC controller.

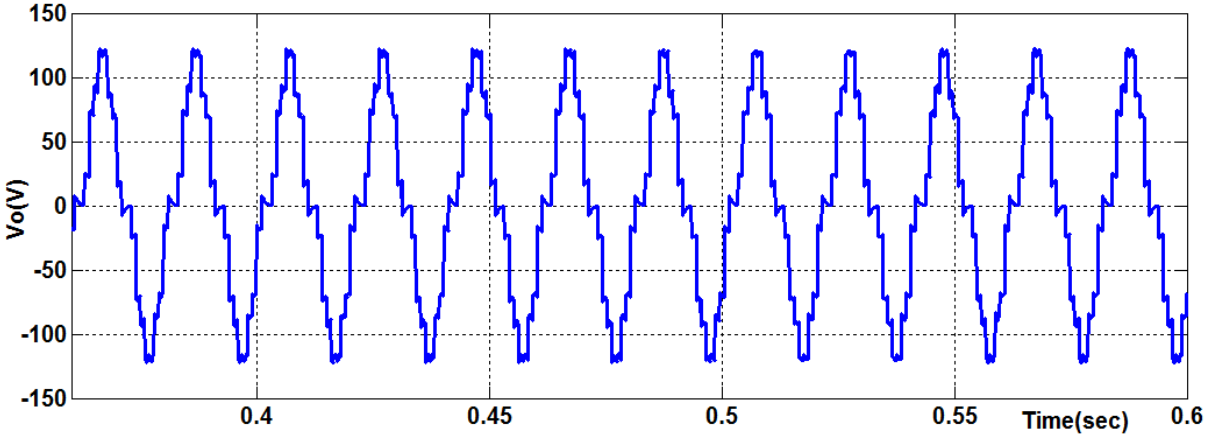

Fig.24 Zoom out of output voltage across motor of closed two-loop QBC-MLI system with PI-HC controller.

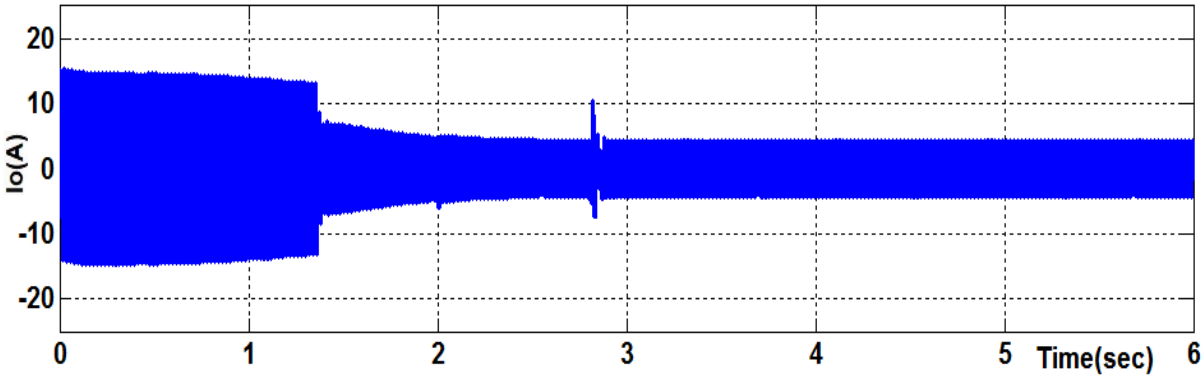

Fig.25 Output current through closed two-loop QBC-MLI system with PI-HC controller

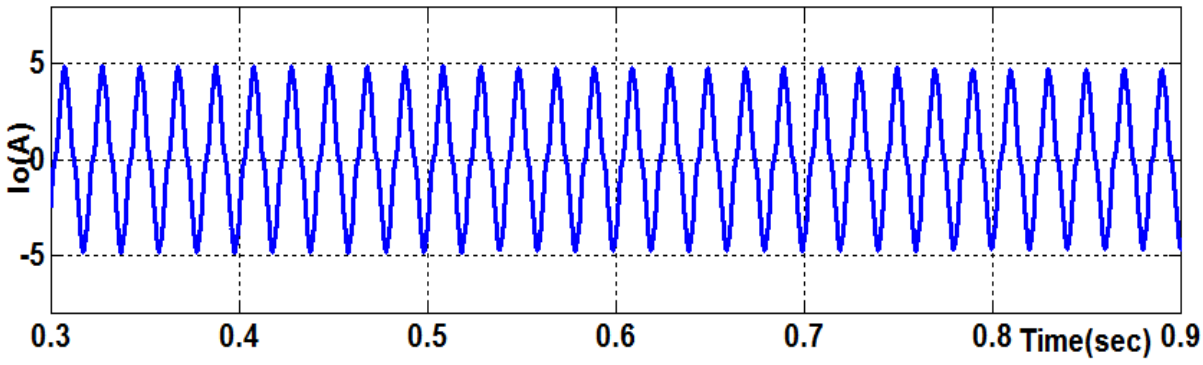

Fig.26 Zoom out of output current through closed two -loop QBC-MLI system with PI-HC controller.

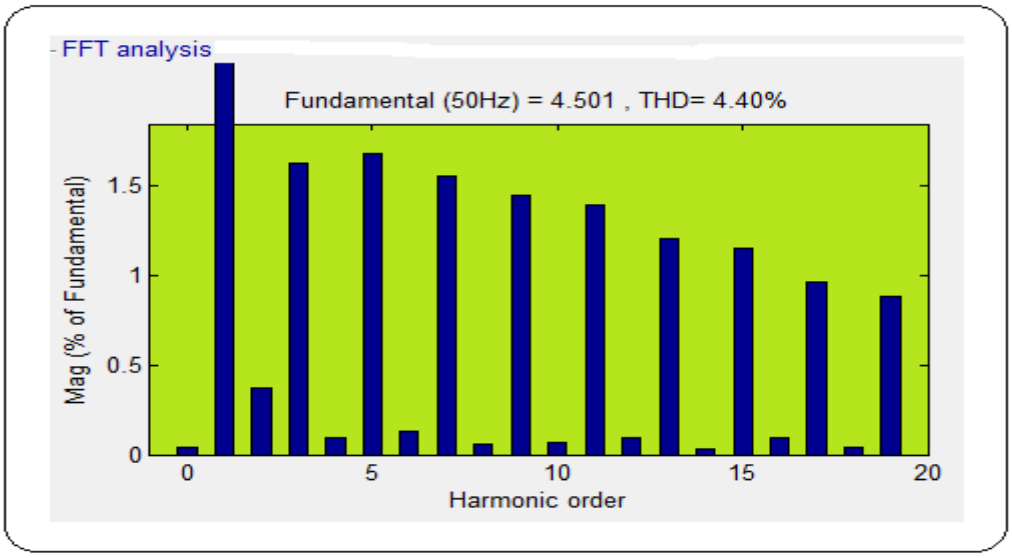

Fig.27 Output current THD with PI-HC controller

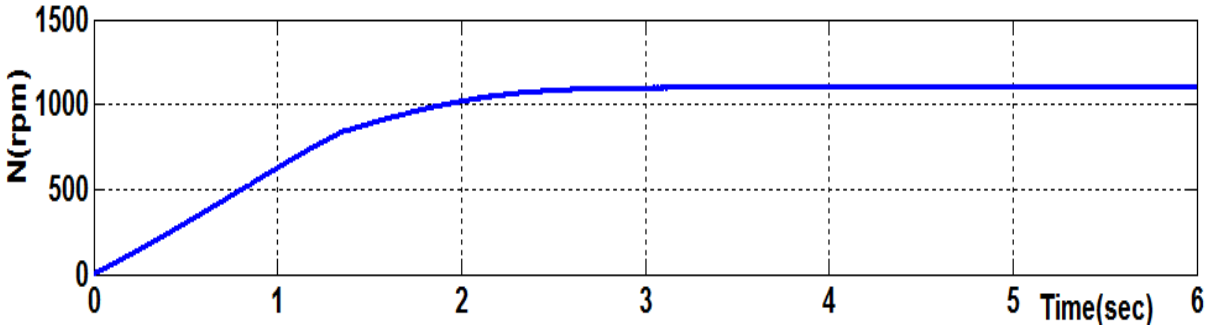

Fig.28 Motor speed of closed two-loop QBC-MLI system with PI controller.

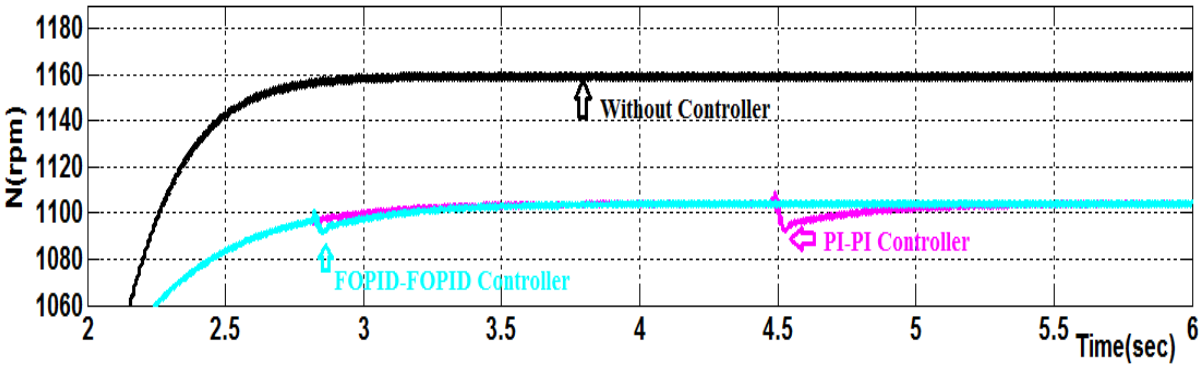

Fig.29 Zoom out of motor speed of closed two-loop QBC-MLI system with PI and HC.

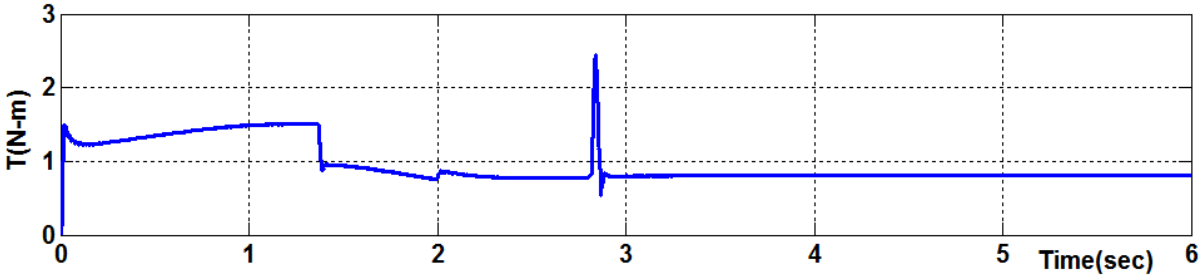

Fig.30 Motor torque of closed two-loop QBC-MLI system with PI-HC controller

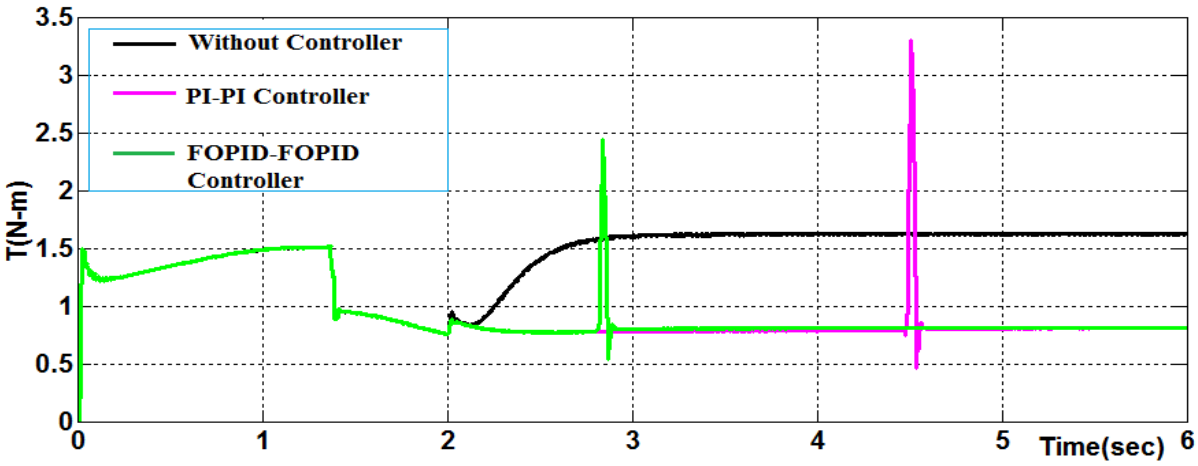

Fig.31 Zoom out of motor torque of closed two-loop QBC-MLI system with PI-HC controller.

Motor speed time-domain characteristics are compared with those of PI-PI and PI-HC controllers in table-1. PI-HC controller reduced the rising time from 2.71s to 2.10s, settling time from 4.91s to 3.12s, and peak duration from 4.50s to 2.82s. From 1.9 rpm down to 0.8 rpm, steady-state error is reduced. Figure 32 shows time domain response bar chart.

Table -1 Comparison of time domain parameters (motor speed) of QBC-MLI using PI and HC controllers

Type of controller	$T_{r(SEC)}$	$T_{p(SEC)}$	$T_{s(SEC)}$	$E_{ss(rpm)}$
PI-PI	**2.71**	**4.50**	**4.91**	**1.9**
PI-HC	**2.10**	**2.82**	**3.12**	**0.8**

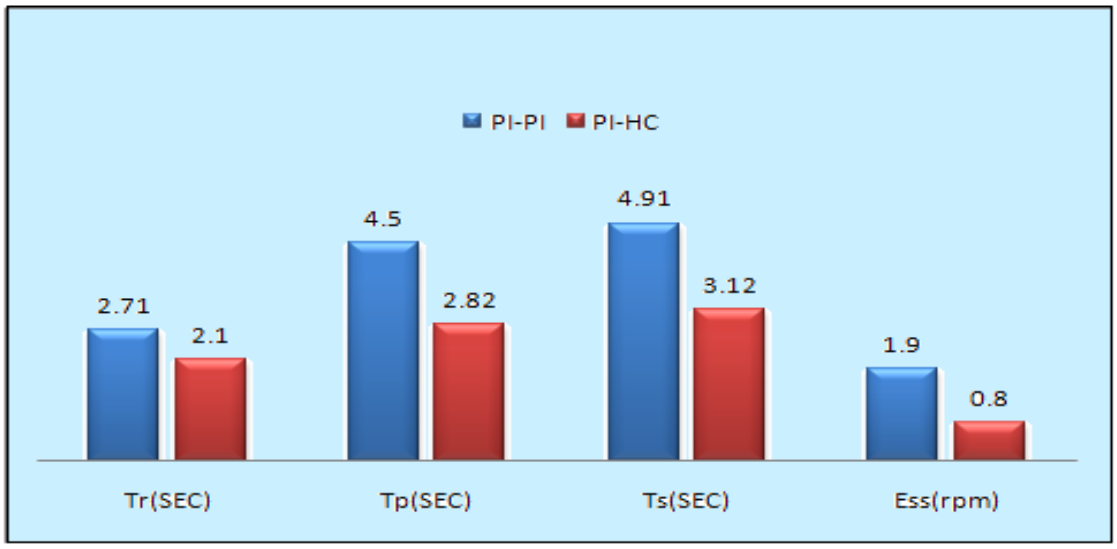

Fig.32. Bar chart PI and HC controller with motor speed response.

Table -2 shows comparison of motor torque response of the PI-HC and PI-PI controllers. Lowering the rising time from 2.1s to 2.0s, settling time from 4.56s to 2.87s, and peak duration from 4.52s to 2.84s. From 0.3 N-m to 0.1 N-m, the steady-state error is reduced. Figure 33 displays time domain response as a bar chart. Table 3 shows the output current and THD of QBC-MLI system with PI and HC controllers. The THD reaction can be observed in Fig.34 as a bar chart. Therefore, compared to a closed 2-loop QBC-MLI system with a PI controller, one with an HC controller is better.

Table -2 Comparisons of time domain parameters (motor torque) of QBC-MLI using PI and HC controllers.

Type of controller	$T_{r(SEC)}$	$T_{p(SEC)}$	$T_{s(SEC)}$	$E_{ss(N-m)}$
PI-PI	**2.1**	**4.52**	**4.56**	**0.3**
PI-HC	**2.0**	**2.84**	**2.87**	**0.1**

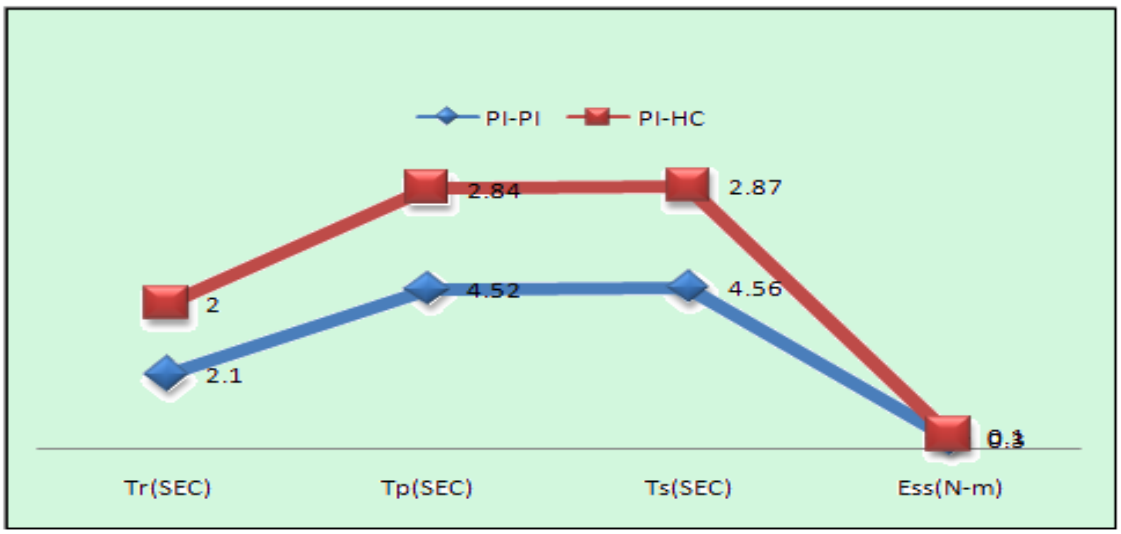

Fig.33. Bar chart PI and HC controller with motor speed response.

Table -3 Comparison of output current THD

QBC-MLI	Output current THD (%)
Without Controller	6.94
With PI Controller	5.34
With HC Controller	4.40

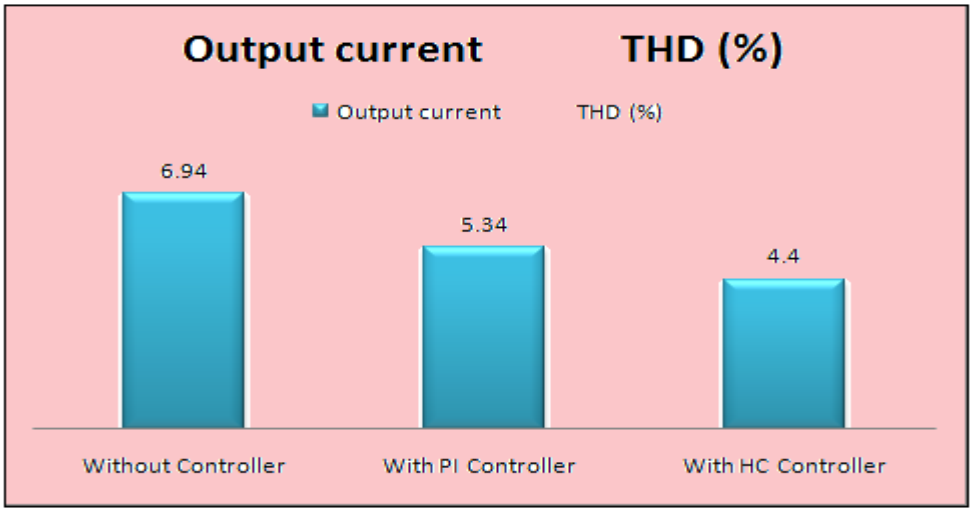

Fig.34 Bar chart of output current THD.

EXPERIMENTAL RESULTS

Fig-35 shows a hardware snapshot of a PV system that uses a single-phase quadratic boost converter and a multi-level inverter. In Figure 36, we can see the voltage across the PV array. The quadratic boost converter's switching pulses for M1 and M2 are illustrated in Fig.37. Fig.38 displays the voltage across the quadratic boost converter. Pulses

for switching S1 and S3 of MLI are shown in Fig.39. Fig. 40 portrays output voltage across the MLI, whereas Fig. 41 portrays output current via the motor load.

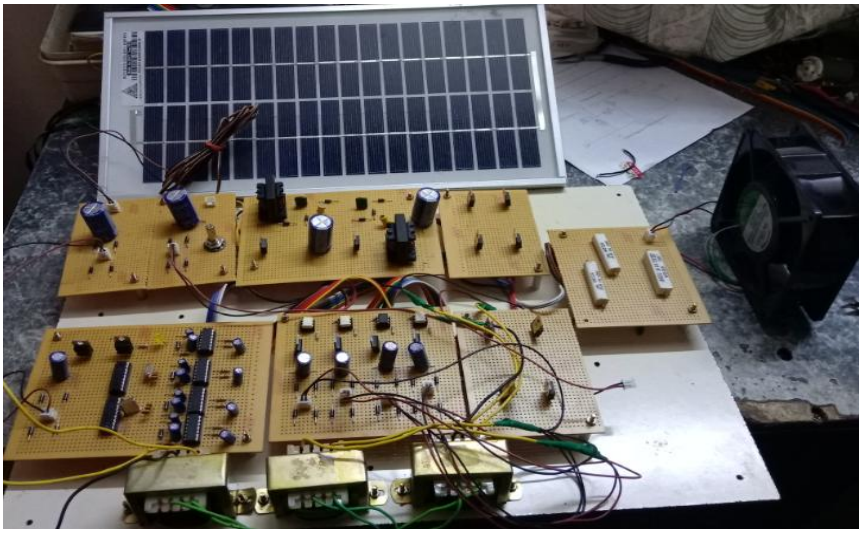

Fig.35 Hardware snapshot of QBC-MLI with motor load

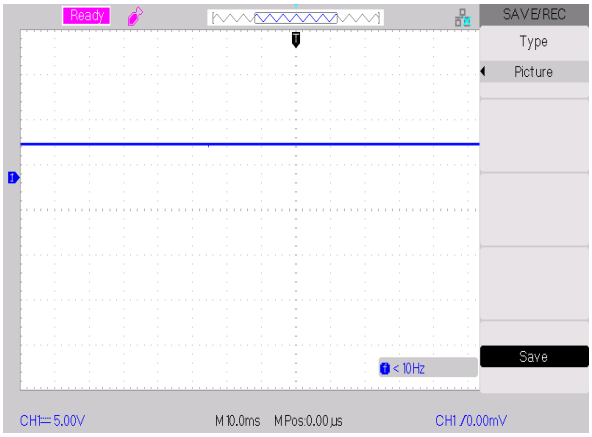

Fig.36 Input voltage

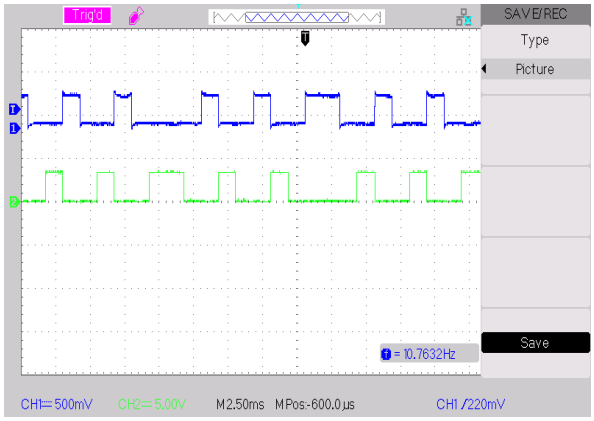

Fig.39 Switching pulses for S1, S3 of MLI

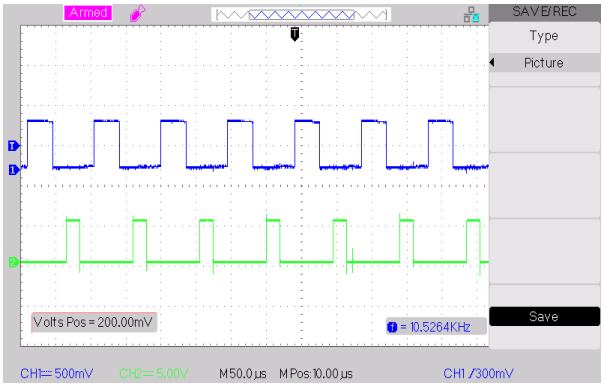

Fig.37 Switching pulses for M1 & M2 of QBC

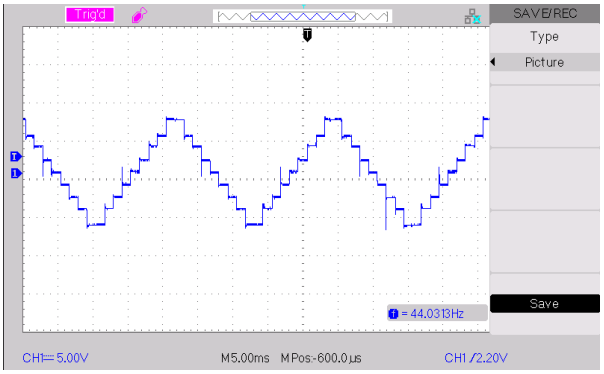

Fig.40 Voltage across motor load

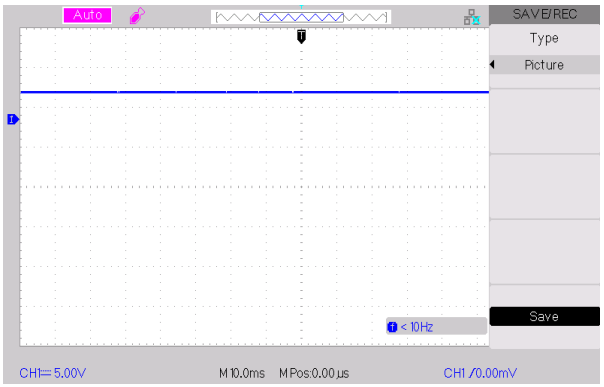

Fig.38 Voltage across QBC

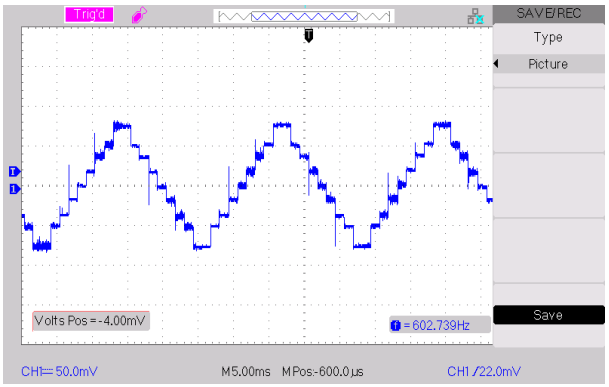

Fig.41 Current through motor load

CONCLUSION

For machine-tool applications using PI-PI and PI-HC controllers, simulation experiments were conducted for both open-loop source disturbance and closed 2-loop QBC-CMLI systems. Findings that were shown were obtained by using models for QBC-CMLI systems that were built in Simulink. In comparison to PI-PI controlled QBC-CMLI system under motor load, results show closed 2-loop PI-HC controlled system provided a lower output current THD and better time responsiveness of motor speed and torque.

Shorter rising and settling times as well as lower steady-state errors in motor speed and torque are most important features of proposed new QBC-CMLI system. Suggested HC-controlled closed-loop QBC-CMLI system exhibits much improved dynamic responsiveness. Our work validates the simulation results with hardware implementation. However, due to cascading process, the suggested QBC-CMLI system shows the enhanced hardware count, which is the downside of this system.

REFRENCES

[1] Y. Li, Z. Zhu, Y. Yang et al., "An input-powered high-efficiency interface circuit with zero standby power in energy harvesting system", J. Power Electron., vol. 15, no. 4, pp. 1131-1138, 2015.

[2] D. Lee, "Simple MOSFET gating delay scheme for SMPS start-up in the standby power reduction circuit," in IET Power Electronics, vol. 11, no. 1, pp. 16-22, 12 1 2018.

[3] S Sreekanth, S Gomathy, "Speed control of a three phase Induction motor using PI Control and Fuzzy logic control Method", International Journal of Emerging Technology and Advanced Engineering, March 2015.

[4] Ramesh Babu, A., T. A. Raghavendiran, V. Sivachidambaranathan, and J. Barnabas Paul Glady. "Novel cascaded H-bridge sub-MLI with reduced switches towards low total harmonic distortion for photovoltaic application." International Journal of Ambient Energy ISSN: 0143-0750, Vol.39, No.2, pp.117-121,Feb.2018.

[5] Xueshan Liu, Jian PIng Xu, Zhangyong Chen, Nan Wan, "Single inductor dual output buck-boost power factor correction converter", IEEE Trans. Ind. Electron., vol. 62, no. 2, pp. 943-952, Feb. 2015.

[6] Rameshbabu A, Ravikumar D N S, Geetha V," Simulation of Single Phase Switching Capacitor 49 Level Inverter with Reduced THD" International Journal of Engineering and Advanced Technology (IJEAT), ISSN:2249-8958,Vol.8,Issue-6, pp.837-841, 2019.

[7] S. Singh, B. Singh, G. Bhuvaneswari, V. Bist, A. Chandra and K. Al-Haddad, "Improved-Power-Quality Bridgeless-Converter-Based Multiple-Output SMPS," in IEEE Transactions on Industry Applications, vol. 51, no. 1, pp. 721-732, Jan.-Feb. 2015.

[8] H.-S. Kim et al., "On/Off control of boost PFC converters to improve light-load efficiency in paralleled power supply units for servers", IEEE Trans. Ind. Electron., vol. 61, no. 3, pp. 1235-1242, Mar. 2014.

[9] Babu, A. Ramesh, and T. A. Raghavendiran. "High voltage gain multiphase interleaved DC-DC converter for DC micro grid application using ıntelligent control." Computers & Electrical Engineering, ISSN:0045-7906, Vol.74, pp.451-465, March 2019.

[10] M. L. Dhola, C. C. Shah, S. L. Kaila, "Power factor improvement using Boost converter", International Journal of Advance Engineering and Research Development (IJAERD), vol. 1, no. 3, pp. 1-4, 2014.

[11] P shanmugasundram, A ramesh babu,"Application of DSTATCOM for loss minimization in radial distribution system" proceedings of the international conference on soft computing systems, advances in intelligent systems and computing, vol.397 pp.189-198, Dec. 2015.

[12] K. Anitha, R. Chatterjee, T. Ramadevi, P. A. Rao, K. Ravikanth, "Analysis of Active Power Factor Correction Using Single and Dual Mode Boost Converter", International Journal of Electrical and Electronics Research, vol. 3, no. 2, pp. 38-44, 2015.

[13] Saravanan, M., and A. Ramesh Babu. "High Power Density Multi-Mosfet-Based Series Resonant Inverter for Induction Heating Applications." International Journal of Power Electronics and Drive Systems (IJPEDS) ISSN: 2088-8694, Vol. 7, No. 1 pp. 107-113, March 2016.